

Experimental and numerical investigation of the splice length requirement in high volume fly ash-self compacting concrete (HVFA-SCC) beam

Rosyid Kholilur Rohman^{1*}, Stefanus Adi Kristiawan^{2*},
Achmad Basuki², Halwan Alfisa Saifullah²

¹ Civil Engineering Doctoral Study Programme, Faculty of Engineering, Sebelas Maret University, Surakarta, 57126, Indonesia

² Department of Civil Engineering, Faculty of Engineering, Sebelas Maret University, Surakarta, 57126, Indonesia

ABSTRACT

This paper aims to determine the required lap splice length of tensile reinforcement embedded in high volume fly ash-self compacting concrete (HVFA-SCC) beams. The lap splice length is governed by the bond strength of the concrete to the reinforcement. Several studies have shown that the bond strength of HVFA-SCC is greater than that of normal concrete (NC). The difference in the bond strength value will affect the lap splice length requirement. In this research, an experimental investigation was carried out on eight beams with dimensions of 150 × 250 mm and a length of 2 m under four points of loading. The beams were designed with various lap splices, i.e., 25%, 50% and 75% of the expected lap splice length. Other beams without lap splice were prepared as a control. A numerical study using ATENA Engineering software was also conducted to extend the investigation covering a longer lap splice length. The analysis results show that a lap splice length of 28.8 d_B produces a flexural capacity equivalent to the control beam, and the tensile reinforcement has reached its yield state. This lap splice length is lower than expected in NC, suggesting that an efficient tensile reinforcement lap splice can be projected in HVFA-SCC beams.


Keywords: Bond strength, HVFA-SCC, Numerical simulation, Splice length.

OPEN ACCESS

Received: August 11, 2023
Revised: December 2, 2023
Accepted: December 11, 2023

Corresponding Author:

Rosyid Kholilur Rohman
rosyid86@student.uns.ac.id
Stefanus Adi Kristiawan
s.a.kristiawan@ft.uns.ac.id

 **Copyright:** The Author(s). This is an open access article distributed under the terms of the [Creative Commons Attribution License \(CC BY 4.0\)](https://creativecommons.org/licenses/by/4.0/), which permits unrestricted distribution provided the original author and source are cited.

Publisher:

[Chaoyang University of Technology](https://www.caoayang.com)
ISSN: 1727-2394 (Print)
ISSN: 1727-7841 (Online)

1. INTRODUCTION

The development of concrete materials technology is progressing rapidly. As a result, several types of concrete have been developed to get better concrete performance during the construction process and post-construction (Dash and Kar, 2018; Kodeboyina, 2018; Thienel and Haller, 2020; Sheen et al., 2021; Unis et al., 2022). One of the concrete types being developed is self-compacting concrete (SCC).

The three main characteristics of SCC are filling ability, passing ability, and segregation resistance. Filling ability is the ability to flow under its weight without any intentional vibration. Passing ability is the ability of concrete to flow through and around reinforcement and other obstacles and maintain its homogeneity. Segregation resistance is the resistance of concrete not to experience segregation when flowing during the self-compaction process (Karthik et al., 2021; Serraye et al., 2021; Ahmad et al., 2023). These properties are possible due to the moderate viscosity of SCC. Therefore, the composition of the SCC contains a higher volume of smaller particles than that of NC. The higher volume of small particle proportions causes the cement volume in SCC generally is higher than in NC. This large amount of cement is a disadvantage, considering that the price of cement is higher than other components. In addition, cement is known as a material that is not environmentally friendly, related to CO₂ emissions generated during

the production process. In the production of 1.0 kg of cement, the amount of CO₂ emissions is equivalent to 0.9 kg (Fayomi et al., 2019). Therefore, reducing the use of cement is needed as a way to make environmentally friendly concrete. One method that can be suggested is replacement some of the cement with fly ash (FA), a by-product of coal burning in thermal power stations. Cement can be replaced with FA in high volumes, even at more than 50% replacement levels. Using FA in larger amounts in the SCC mixture can decrease greenhouse gas emissions from cement production by half as the demand for cement decreases. SCC with FA content above 50% as a substitute for cement is known as High Volume Fly Ash-Self Compacting Concrete (HVFA-SCC). This particular type of concrete has been shown by several researchers to have properties that allow its application as a structural element (Budi et al., 2021; Zhou et al., 2021; Rohman et al., 2023).

Meanwhile, in the construction of concrete structures, the availability of reinforcements is often shorter than the required length for structural elements of reinforced concrete. This situation forced the construction workers to carry out reinforcement splicing. One method that is widely applied in the field is the lap splice method. The lap splice length must be carefully calculated so that the full stress transfer mechanism occurs. The lap splice length is closely related to the development length to ensure that the reinforcing steel can develop its strength up to its yield limit. If the lap splice length is insufficient, slippage failure will occur and cause the reinforcement not to develop its full strength (Gillani et al., 2021).

The development length and the lap splice length are governed by the bond of the concrete to the reinforcement. A good bond strength will ensure that an effective load transfer to the reinforcement can be expected until reaching its yield limit (Arezoumandi et al., 2018). The bond strength is influenced by three factors, namely chemical adhesion, frictional force, and mechanical interlock (Hu et al., 2020). Several studies have shown that the splice length influences the bond strength value. The longer the splice length, the smaller the bond strength between concrete and reinforcing steel. Insufficient splice length causes bond failure in the spliced beam (Gillani et al., 2021; Rohman et al., 2022).

Previous studies indicated a difference in the bond strength between various concrete types, so a difference in the required lap splice length between various concrete types can be expected. For example, Zheng et al. (2021) compared the bond strength between NC and HVFA-SCC with pull-out testing. The reinforcement used is Glass Fiber Reinforced Polymer (GFRP). The results of this research stated that the bond strength could be increased using HVFA-SCC instead of NC. Another study has shown that the HVFA-SCC bond strength is greater than NC and SCC bond strength (Rohman et al., 2022). Meanwhile, El-Azab and Mohamed (2014) conducted a study on the required lap splice length of reinforcement in High Strength Concrete (HSC) beams with a compressive strength of 75 MPa. The findings revealed that HSC beams with a splice length of 40

d_B were able to withstand loads equivalent to beams without a splice length. Furthermore, El-Azab et al. (2014) also conducted a similar study using High Strength-Self Compacting Concrete (HS-SCC). A minimum splice length of 40 d_B in the HS-SCC beam was needed to achieve a maximum load equivalent to the control beam.

Research focusing on determining the required lap splices length in HVFA-SCC beams is still very limited. Alghazali and Myers (2019) conducted one related study on HVFA-SCC splice beams. FA content of 50%, 60% and 70% was used as a cement replacement. The beams were designed with a lap splice length of 254 mm (13.4 d_B) to ensure failure occurred at the splice before the reinforcement yielded. The results showed an increase in bond efficiency with a higher FA content. However, the study did not include determining the required lap splice length to achieve maximum force equivalent to a beam without a lap splice.

Another related study on splice beams was conducted by Kristiawan et al. (2022) using High Strength-High Volume Fly Ash-Self Compacting Concrete (HS-HVFA-SCC) with a compressive strength of 73 MPa. The study involved variations in lap splice length ranging from 34.2 to 57 d_B using plain reinforcement. The findings showed that the flexural load behaved similarly to a non-spliced beam when using plain reinforcement with a splice length of 38 d_B . However, no study has been conducted yet on investigating the required splice lengths for HVFA-SCC beams with deformed reinforcements to meet a similar performance to that of non-splicing beams. Therefore, this research aims to determine the required lap splice length of deformed tensile reinforcement embedded in the HVFA-SCC beams based on the flexural performance criteria. The research is conducted through experimental tests in the laboratory and numerical simulations using 3D ATENA Engineering software version 5.7 to achieve that goal. The numerical models of the ATENA software are first validated by comparing the results of the laboratory experiments with the numerical simulations regarding crack patterns in the investigated beams, failure modes, load versus deflection behaviors, and reinforcement steel stress values at the lap splice zone. The numerical simulation is then used to expand the variables that need to be investigated to determine the required lap splice length in the HVFA-SCC beam, resulting in an equivalent flexural performance to that in the control beam.

2. MATERIALS AND METHODS

2.1 Materials and Properties

HVFA-SCC is made with a compressive strength of 30 MPa. A trial mix has been carried out to obtain an appropriate composition meeting the requirements of SCC. A superplasticizer (i.e., Consol P 292 As), which belongs to the Modified Carboxylate (MP) type, is added. The composition of the concrete mixture is shown in Table 1.

A compressive strength test was carried out on a

cylindrical concrete specimen with a diameter of 150 mm and a height of 300 mm, according to ASTM C 39 (2001). The test was conducted at the specimen's age of 28 days. The obtained average compressive strength of concrete (f_c') is 33 MPa. In addition, a tensile test was conducted using the Universal Testing Machine (UTM) to determine the yield (f_y) and ultimate (f_u) strength of the reinforcing steel used. The tensile reinforcement was deformed reinforcement with a diameter of 16 mm. Meanwhile, the compression reinforcement and stirrups used plain bar with a diameter of 8 mm. The results of the tensile reinforcement test can be seen in Table 2.

Table 1. Concrete mixture proportion

Material	Type	Weight (kg)
Cement	1	275
FA	C	275
Fine aggregate	River sand	635
Coarse aggregate	Crush stone	876
Water	NA	176
Superplasticizer	MP	5.5

Table 2. Reinforcement property

Diameter (mm)	Effective diameter (mm)	Yield strength (MPa)	Ultimate strength (MPa)
8	7.70	340	470
16	15.62	415	582

The pull-out test is used to determine the bond strength value between HVFA-SCC and the reinforcement. The specimens for this test refer to RILEM (1994), which are cubes with a size of 200 mm. The reinforcement used in the pull-out test was reinforcing steel with a 16 mm diameter embedded in the concrete specimens. The embedded reinforcement was $5 d_B$ or 80 mm long. There was no contact between the concrete and the reinforcement at the top of the specimen because a PVC pipe was inserted in this part of the specimen. The setup of pull-out testing can be seen in Fig. 1.

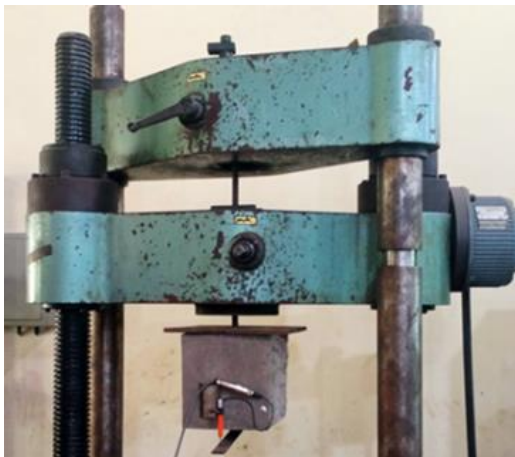


Fig. 1. Pull-out testing

The pull-out test was conducted by pulling the reinforcing bar using the UTM tool until the maximum force was obtained. The value of the applied force (P) and the amount of slip between the concrete specimen and the reinforcing bar were recorded during the test. The P value at the time of slip of 0.25 mm is called the critical force (P_{cr}). The critical force value is used to determine the critical bond strength. The results of critical bond strength between concrete and reinforcing steel is 3.05 MPa, while the maximum nominal bond strength is 12.09 MPa. The relationship curve between bond strength vs. slip can be seen in Fig. 2. Bond strength vs. slip data from the pull-out test results will be used as bond reinforcement input in numerical simulations with the ATENA Engineering software.

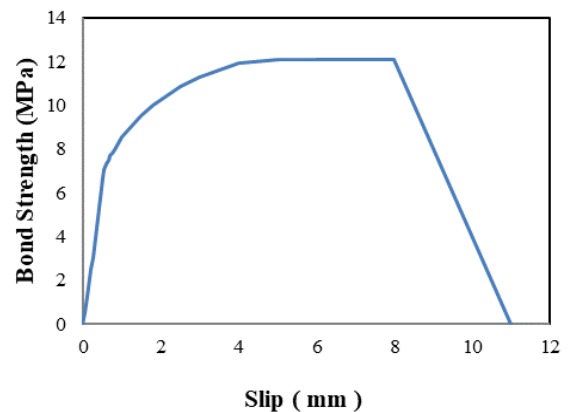


Fig. 2. Bond strength vs. slip

2.2 Beam Specimens

Beam test specimens were 150 mm wide, 250 mm high and 2000 mm long. Two tensile reinforcements were provided with deformed bars of 16 mm diameter in the tensile zone of the beams. Additionally, plain bars of 8 mm diameter were used as compression reinforcements and stirrups. The thickness of the bottom concrete cover (c_b) and side concrete cover (c_o) were 20 mm, respectively. The stirrups were installed along the shear span at a distance of 70 mm. The length of the lap splice on the beam test specimens was established based on the bond strength value from the pull-out test that had been done previously. The bond strength value used the critical bond strength of 3.05 MPa.

The development length is the length of reinforcement that needs to be embedded into the concrete to develop its full tensile strength. The following formula calculates the development length (l_s):

$$l_s = \frac{f_y}{4u} d_B \quad (1)$$

where f_y is yield stress, u is bond strength and d_B is diameter of reinforcing steel.

The maximum splice length was determined by 75% of the development length (l_s) calculated from Equation (1). The other splice length was determined at 50% and 25% l_s . The assigned splice length was intended to induce a splitting or slippage failure in the experiment.

Table 3 shows four types of the beam specimens. B-0-16 denotes a 16 mm diameter reinforced concrete beam without lap splice. The other beams are reinforced beams with a diameter of 16 mm and lap splice lengths (l_d) varying from 140, 300 and 400 mm. Two beam specimens were made for each beam type so that eight beams were tested. The sketch of the concrete beam specimens can be seen in Fig. 3.

Table 3. Beam specimens

Specimens	f_c (MPa)	f_y (MPa)	b (mm)	h (mm)	d_B (mm)	l_d (mm)
B-0-16	33	415	150	250	15.6	-
B-140-16	33	415	150	250	15.6	140
B-300-16	33	415	150	250	15.6	300
B-400-16	33	415	150	250	15.6	400

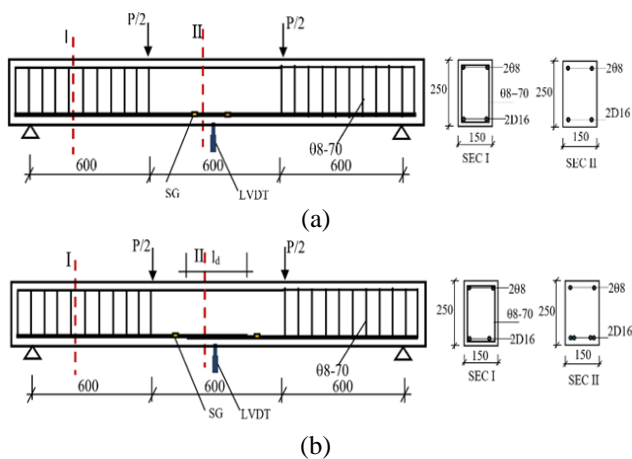


Fig. 3. (a) Control beam (b) splice beam with their reinforcements detail

2.3 Experimental of Beam Specimens

Beam testing is carried out by providing 4-point loadings. The applied concentrated load was distributed to the beam through the load transfer steel beam. The distance between the 2-point loads was 600 mm long. The distance between the concentrated load and the closest support was 600 mm. The load was observed by the load cell placed in the mid-span of the load transfer beam. A strain gauge was installed at the end of the lap splice and read by a strain indicator. The deflection of the beam at mid-span was measured by 2 LVDTs installed on both sides of the beam. Load, strain, and displacement readings were recorded on the data logger. Cracks due to loading are marked on the beam surface every interval loading of 5 KN.

2.4 Numerical Simulations

The numerical simulation in this research was provided using finite element method software ATENA 3D engineering version 5.7. This software was used to simulate the behavior of splice beams under flexural loading, including the crack pattern, failure modes, concentrated load at the point loading, mid-span displacements, and reinforcing steel stresses.



Fig. 4. Setup of beam testing

The concrete material in this study is modeled as a fracture-plastic constitutive model with the material type CC3DNonlinCementitious, where non-linear behavior is explained based on the uniaxial stress-strain relationship. The uniaxial stress-strain curve of concrete in compression, presented in Fig. 5, is divided into four parts indicating the state of damage in concrete. The behavior of concrete in tension before cracking is linearly elastic, as shown in Fig. 5, part 1. Then part 2 illustrates the effect of crack propagation using a fictitious crack model based on crack-opening law and fracture energy on stress-strain relationship. The behavior of concrete before maximum compressive strength is assumed to be hardening, as displayed in part 3, and then softening, as presented in part 4.

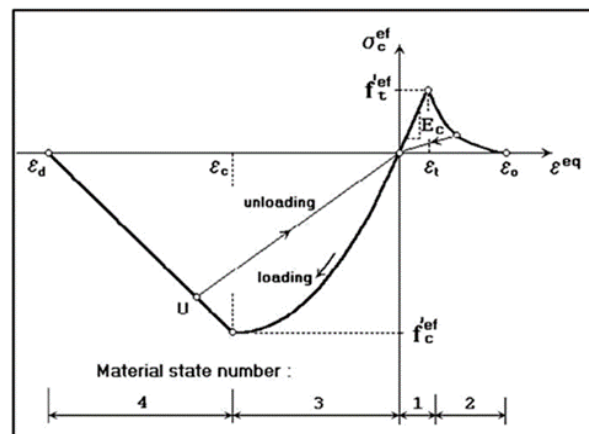


Fig 5. Concrete uniaxial stress-strain relationship

The constitutive reinforcement model follows perfectly elastic-plastic behavior and is defined through the applied stress-strain relationship, namely bilinear with hardening. The loading on the beam was prescribed deformation. The solution parameter used was the Newton-Raphson Method so that the resulting solution path remains constant in observing the entire load-deflection relationship (Elkheshen et al., 2022). The iteration limit process was 140 iterations. Fig. 6 shows an outline of the test object of the beam with modeling using the ATENA Engineering software.

The adopted meshing was brick with a size of 50×50 mm. The material properties were adjusted to represent the experimental test data, such as the compressive strength of the cylinder concrete of 33 MPa. Other input parameters used the default values from ATENA Engineering software. Monitoring was carried out at two main points to generate the load-deflection curve. The first point is to monitor the deflection located in the middle of the beam span, and the second is to monitor the load located at the steel plate under the loading point. Numerical simulations were carried out on all types of beams in Table 3 and extended with splice lengths of 450 and 500 mm.

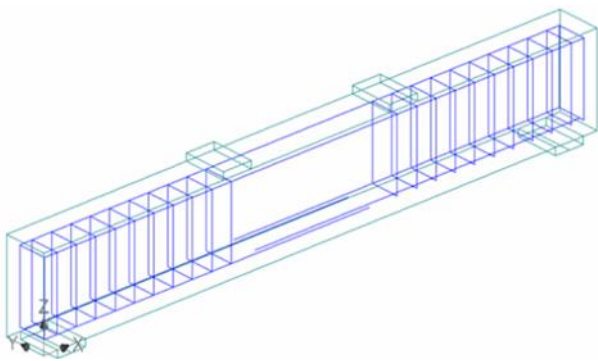


Fig. 6. Structure model of splice beam with ATENA engineering software

3. RESULTS AND DISCUSSION

3.1 Crack Pattern and Failure Mode

The crack pattern on the control beam due to the applied load is shown in Fig. 7. The crack that appears is a flexural crack with a vertical direction. The first location of the flexural crack is seen in the mid-span (in the constant moment area). As the load increases, vertical cracks develop into the compression zone. In the control beam, the given load resulted in the tensile reinforcement to yield and is followed by the destruction of the concrete in the compression zone. The test results show that the failure that occurs is the flexural failure mode. From Fig. 7, it can be seen that the beam crack pattern from the numerical simulation and the experimental results are almost the same.

Figs. 8, 9 and 10 show the beam's crack pattern with lap splices in the the mid-span. In all splice beams, a first flexural crack occurs at the ends of the lap splice. As the

load increases, additional flexural cracks form outside the constant moment area. When the load is added to about 85% of the maximum load, horizontal cracks form around the lap splices. The additional load further exacerbates these horizontal cracks so that, in the end, the concrete cover experiences splitting. From Figs. 8, 9 and 10, it can be seen that the beam crack patterns of the numerical simulation and the experimental results are almost the same, and the failure that occurs is splitting failure.

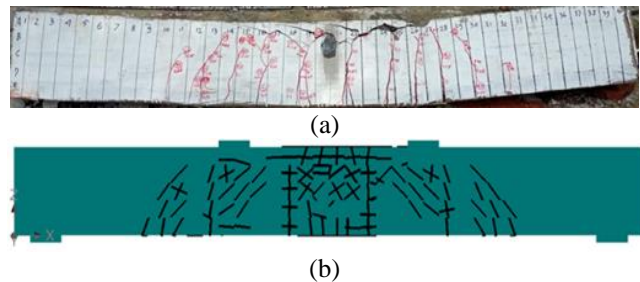


Fig. 7. Crack pattern of control beam (a) test results (b) numerical simulation results

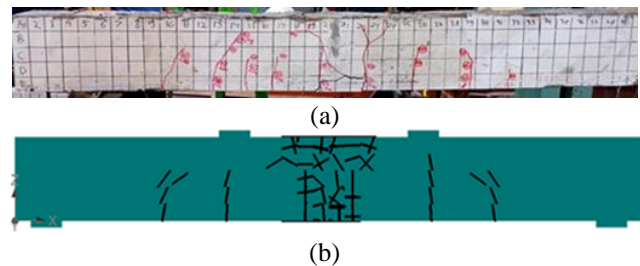


Fig. 8. Crack pattern of B-140-16 (a) test results (b) numerical simulations results

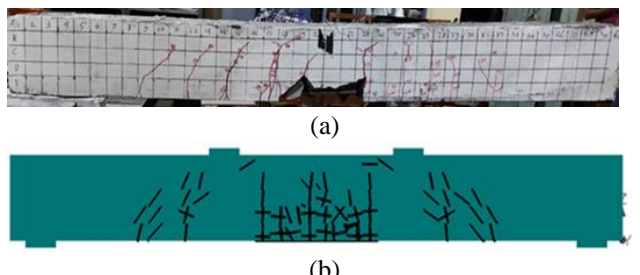


Fig. 9. Crack pattern of B-300-16 (a) test results (b) numerical simulations results

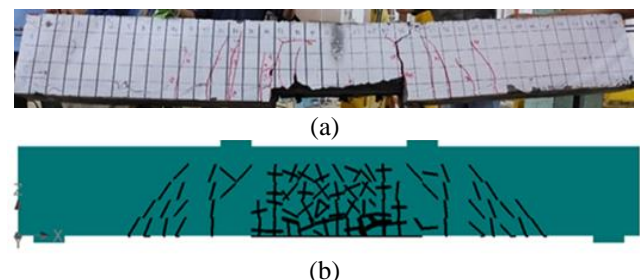


Fig. 10. Crack pattern of B-400-16 (a) test results (b) numerical simulations results

3.2 Load vs. Displacement

Fig. 11 shows the relationship between load vs. displacement on each beam. Load vs. displacement on each beam has almost the same pattern, forming a trilinear curve: the more the load increases, the greater the displacement in the mid-span of beam specimens.

At the beginning of loading, until the first crack occurs in the control beam (B-0-16), i.e., at a load of about 25 kN, the curve forms the first linear relationship between load and displacement. After the load at the first crack is exceeded, the curve will bend and show a second linear relationship between load and displacement until 85% of the maximum load, where the third linearity of the curve begins. The third linear relationship can be observed where a small increase in loading causes a larger displacement value until failure occurs. The next section shows that reinforcement strain reaches a yielding state at this stage.

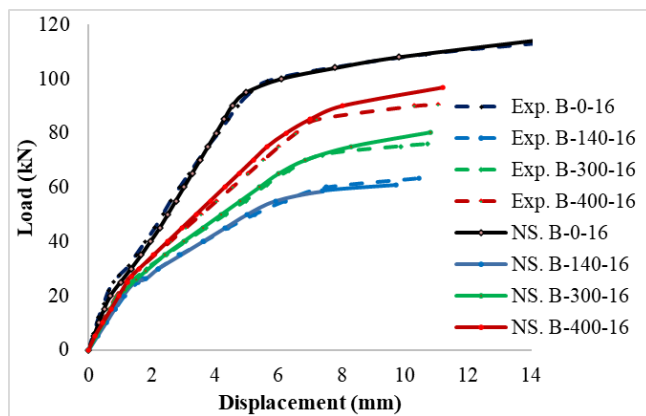


Fig. 11. Load vs. displacement comparison between experimental (Exp) and numerical simulations (NS)

In the splice beams, the load vs. displacement also shows a trilinear relationship. The curve shows the first linear relationship between load and displacement, starting at the beginning of loading until the first crack occurs. After the first crack load has been exceeded, the curve will bend and show a second linear relationship until 95% of the maximum load, where a drastic increase in the reinforcing steel strain begins. This increase in reinforcing steel strain is due to wider cracks, especially at the ends of the lap splice. After the limit of the second linear curve is exceeded, a third linear relationship can be observed from a significant increase in the displacement value at a moderate increase in load. In this third phase, the intensity and width of the cracks increase, triggering the transfer of stress to the reinforcement, causing the strain on the reinforcing steel to increase drastically. However, the reinforcement strain does not reach a yielding state, as shown in the next section.

It can be seen in Fig. 11 that the load vs. deflection graph of the numerical simulation (NS) results also shows a trilinear pattern. The difference between the experimental and numerical simulation results is less than 10%.

3.3 The Reinforcement Stress

The stress value of the reinforcing steel can be calculated from the resulting strain value. The steel strain is obtained from the reading of the strain indicator. The reinforcing steel stress is obtained from the strain that occurs multiplied by the steel modulus of elasticity (E_s). The modulus of elasticity for steel reinforcement is 200 GPa.

The reinforcement stress can also be obtained from numerical simulation results using ATENA software. Furthermore, numerical simulations were also carried out by adding beams with lap splice length of 450 and 500 mm. The results of calculating steel stress from experimental results and numerical simulation are presented in Table 4.

Table 4. Reinforcement stress of splice beam

Specimen	d_B	l_d	l_d/d_B	$f_{s_{exp}}$	$f_{s_{numeric}}$	$f_{s_{exp}}/f_{s_{numeric}}$
B-0-16	15.6	-	-	418	415	1.007
B-140-16	15.6	140	9.0	274	246	1.114
B-300-16	15.6	300	19.2	326	304	1.072
B-400-16	15.6	400	25.6	387	386	1.003
B-450-16	15.6	450	28.8	-	415	-
B-500-16	15.6	500	32.1	-	430	-

Table 4 compares the experimental results of steel stress and the results of numerical simulations with ATENA Engineering software. Both analysis results show that the steel stress in the control beam reached the yield stress, while the stress in the splice beam did not reach the yield stress. The longer the lap splice, the greater the stress in the reinforcing steel. This shows that a sufficient lap splice in the beam will ensure the reinforcing steel can fully take a stress up to yield value. The maximum difference between the experimental and numerical simulation results is 11.4%, which occur in beam B-140-16. In general, the numerical simulation with ATENA software can be used to predict the stresses that occur in the reinforcing steel. From the results of the numerical simulation in Table 4 above, it is also seen that at the splice length of $28.8 d_B$ causing the reinforcing steel reached the yield stress. The occurrence of reinforcement yield stress indicates a good stress transfer from the spliced reinforcement and surrounding concrete. The analysis results also show that the stress in the reinforcing steel can exceed the yield stress in the splice length of $32.1 d_B$.

From Table 4, it can be seen that the reinforcement steel stress increases with increasing splice length. Beams with splice lengths of 9.0, 19.2, 25.6, 28.8 and $32.1 d_B$ can reach steel stresses of 246 MPa (59.3% f_y), 304 MPa (73.3% f_y), 386 MPa (93.0% f_y), 415 MPa (100% f_y) and 430 MPa (103.6% f_y), respectively. In a beam with a splice length of $28.8 d_B$, the steel stress can reach the yield stress so that a splice length of $28.8 d_B$ can be concluded as the required splice length.

3.4 The Flexural Capacity

The flexural capacity of the beam can be known from the maximum load (P_{max}) that the beam can carry. The maximum load of the beam from the experimental results and numerical simulations is presented in Table 5, while the P_{max} of the numerical simulation results vs. l_d/d_B is presented in Fig. 12. From the comparison between the experimental results and the numerical simulation results, it can be seen that the ratio of the experimental results and the numerical simulation is between 0.934 and 1.039. The difference between the two analysis results is less than 5%.

From Table 5, it can be seen that the maximum load increases with increasing splice length. The maximum load on the control beam is 116.23 KN. Beams with splice lengths of 9.0, 19.2, 25.6, 28.8 and 32.1 d_B can reach maximum loads of 60.99, 80.24, 96.76, 115 and 132.4 KN, respectively. The maximum load values of the splice beam with 9.0, 19.2, 25.6, 28.8 and 32.1 d_B when compared with the maximum of the control beam are 52.5%, 69%, 83.2%, 99% and 113.9% of the P_{max} of the control beam.

Beams with splices length 9.0, 19.2 and 25.6 d_B have a lower capacity than the control beam. Beams with splices length 28.8 d_B can withstand loads equivalent to beams without lap splices length (control beam). The beam with a splice length of 32.1 d_B could withstand a greater load than the control beam. Beams with sufficient splice length could withstand a load equal to that of the control beam and even exceed the control beam's maximum capacity. Beams with sufficient splice length will increase the bond strength value so that the reinforcement can fully take load up to yield value without being preceded by splitting, as in the case of the beam with insufficient lap splice length. Consequently, a minimum splice length has to be provided to obtain spliced beam with a similar capacity to the control beam. In this research, the required splice length is 28.8 d_B .

The required splice length is influenced by bond strength. The greater the bond strength, the shorter the required splice length. Several studies show that the bond strength of HVFA-SCC is greater than that of NC (Zheng et al., 2021; Rohman et al., 2022). Therefore, the required splice length for HVFA-SCC will be shorter than NC.

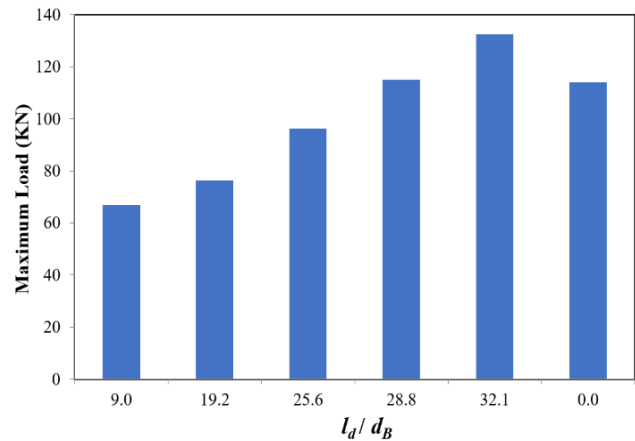


Fig. 12. P_{maks} vs. l_d/d_B (numerical simulations)

3.5 Comparison with Normal Concrete (NC)

The analysis of flexural capacity shows that the splice beam with a splice length of 28.8 d_B is equivalent to that of the control beam. The results of the steel stress analysis also show that at a splice length of 28.8 d_B , the reinforcing steel has reached its yield stress. From the results of the two analyses, it can be concluded that for the HVFA-SCC beam, the required splice length is 28.8 d_B .

ACI 318-19 has formulated the development length for NC. The equation that can be used is:

$$\frac{l_d}{d_b} = \frac{1}{1.1} \frac{f_y}{\lambda \sqrt{f'_c}} \frac{\psi_t \cdot \psi_e \cdot \psi_s \cdot \psi_g}{\left(\frac{c + K_{tr}}{d_b}\right)} \quad (2)$$

where c = the smallest value between thickness of concrete cover, d_b = diameter of reinforcement, l_d = development length, K_{tr} = confinement factor, λ = concrete type factor, f'_c = compressive strength, ψ_e = coating factor, ψ_t = bar casting position factor, ψ_g = reinforcing steel quality factor, and ψ_s = reinforcement size factor.

With data from laboratory tests that have been carried out, namely concrete compressive strength, f'_c , 33 MPa, reinforcing steel yield stress, f_y , 415 MPa, minimum concrete cover thickness of 20 mm, and reinforcement diameter of 15.6 mm, using the equation from ACI 318-19 above will obtain the splice length requirement of 41.05 d_B . Thus, the required splice length for HVFA-SCC beams is shorter than that for NC beams, with a difference of about 29.84%. The required splice length for HVFA-SCC is about 70% of the splice length requirement for NC.

If we calculate the splice length for the HVFA-SCC beam using Equation (2), the calculated result will be longer than

Table 5. Maximum load of beam testing

Specimen	d_B	l_d	l_d/d_B	P_{exp} (KN)	$P_{numeric}$ (KN)	$P_{exp}/P_{numeric}$
B-0-16	15.6	0	0	113.60	116.23	0.977
B-140-16	15.6	140	9.0	63.4	60.99	1.039
B-300-16	15.6	300	19.2	75.8	80.24	0.945
B-400-16	15.6	400	25.6	90.4	96.76	0.934
B-450-16	15.6	450	28.8	-	115.0	-
B-500-16	15.6	500	32.1	-	132.4	-

The results of this study indicate that the required splice length for HVFA-SCC beams is shorter than that of HS-HVFA-SCC beams, which is 38 d_B (Kristiawan et al., 2022). According to El-Azab and Mohamed (2014), it is also shown that the required splice length for HSC beams are longer, which is 40 d_B . Other studies also show that the required splice length for HS-SCC is 40 d_B (El-Azab et al., 2014). It can be concluded that the type of concrete affects the required splice length.

required. This difference is due to the formulation of splice length in ACI 318-19 code referring to the research results on NC. The splice lengths that are too long are not cost-effective in terms of material.

4. CONCLUSION

Based on experimental data and the results of numerical simulations that have been carried out, it can be concluded that the failure on the control beam is flexural failure, while the failure that occurs on the beam with insufficient splice length is splitting. In the splice beam, the greater the lap splice length, the greater the maximum load and reinforcement stress. This shows that the lap splice length affects the stress transfer in the reinforcing steel, thereby increasing the flexural capacity of the spliced beam.

The minimum splice length of tensile reinforcement in the HVFA-SCC beam to produce a similar flexural performance to the control beam is 28.8 d_B . This value represents about 70% compared to the splice length of a NC beam. Therefore, the use of HVFA-SCC in construction will be more efficient.

ACKNOWLEDGMENT

The authors sincerely thank all the HVFA-SCC research team who participated and fully supported the experimental and numerical modeling works. The publication of this manuscript is supported by HGR 2023 (Contract Number: 228/UN27.22/PT.01.03/2023).

REFERENCES

- Ahmed, H.U., Mahmood, L.J., Muhammad, M.A., Faraj, R.H., Qaidi, S.M.A., Sor, N.H, Mohammed, A.S., Mohammed, A.A. 2022. Geopolymer concrete as a cleaner construction material : An overview on materials and structural performances. *Elsevier-Cleaner Materials*, 5, 1–18.
- Ahmad, J., Zhou, Z., Deifalla, A.F. 2023. Steel fiber reinforced self-compacting concrete: A comprehensive review. *International Journal of Concrete Structures and Materials*, 17, 1–22.
- Alghazali, H.H., Myers, J.J. 2019. Bond performance of high-volume fly ash self-consolidating concrete in full-scale beams. *ACI Structural Journal*, 116, 161–170.
- Arezoumandi, M., Steele, A.R., Volz, J.S. 2018. Evaluation of the bond strengths between concrete and reinforcement as a function of recycled concrete aggregate replacement level. *Elsevier-Structures*, 16, 73–81.
- ASTM C 39. 2001. Standard test method for compressive strength of cylindrical concrete specimens. *ASTM Standard Book*, 04, 1–5.
- Budi, A.S., Safitri, E., Sangadji, S., Kristiawan, S.A. 2021. Shear strength of HVFA-SCC beams without stirrups. *MDPI Journal-Buildings*, 11, 1–20.
- Dash, S., Kar, B. 2018. Environment friendly pervious concrete for sustainable construction. In *IOP Conference Series: Materials Science and Engineering*, 410, 012005, 1–10.
- El-Azab, A., Mohamed, H.M. 2014. Effect of tension lap splice on the behavior of high strength concrete (HSC) beams. *HBRC Journal*, 10, 287–297.
- El-Azab, M.A., Mohamed, H. M., Farahat, A. 2014. Effect of tension lap splice on the behavior of high strength self-compacted concrete beams. *Alexandria Engineering Journal*, 53, 319–328.
- Elkhesheh, M., Eltahawy, R., Shedid, M., Abdelrahman, A. 2022. Numerical verification for concrete beams reinforced with CFRP subjected to pure torsion. *Elsevier-Engineering Structures*, 268, 1–20.
- Fayomi, G.U., Mini, S.E., Fayomi, O.S.I., Ayoola, A.A. 2019. Perspectives on environmental CO₂ emission and energy factor in cement industry. *IOP Conference Series: Earth and Environmental Science*, 331, 1–6.
- Gillani, A.S.M., Lee, S.G., Lee, S.H., Lee, H., Hong, K.J. 2021. Local behavior of lap-spliced deformed rebars in reinforced concrete beams. *MDPI Journal-Materials*, 14, 2–15.
- Hu, A., Liang, X., Shi, Q. 2020. Bond characteristics between high-strength bars and ultrahigh-performance concrete. *Journal of Materials in Civil Engineering*, 32, 04019323
- Karthik, D., Nirmalkumar, K., Priyadarshini, R. 2021. Characteristic assessment of self-compacting concrete with supplementary cementitious materials. *Construction and Building Materials*, 297, 123845.
- Kodeboyina. 2018. High performance self-consolidating cementitious composites. CRC Press. London. UK.
- Kristiawan, S.A., Rohman, R.K., Ferdian, E. 2022. Flexural performance of reinforced HS - HVFA - SCC beam with spliced plain bar. *SN Applied Sciences Journal*, 36, 1–12.
- RILEM. 1994. RILEM Technical Recommendations for the testing and use of construction materials. CRC Press. London. UK.
- Rohman, R.K., Kristiawan, S.A., Saifullah, H.A., Basuki, A. 2022. Reinforcement to concrete bond strength : A comparison between normal concrete and various types of concrete. *IOP Conference Series: Journal of Physics*, 2190, 1–8.
- Rohman, R.K., Kristiawan, S.A., Basuki, A., Saifullah, H.A. 2023. Bond strength between reinforcement and high volume fly ash-self compacting concrete (HVFA-SCC). *IOP Conference Series: Earth and Environmental Science*, 1195, 1–9.
- Serraye, M., Kenai, S., Boukhatem, B. 2021. Prediction of compressive strength of self-compacting concrete (SCC) with silica fume using neural networks models. *Civil Engineering Journal (Iran)*, 7, 118–139.
- Sheen, Y., Le, D., Lam, M.N. 2021. Performance of self-compacting concrete with stainless steel slag versus fly

- ash as fillers: A comparative study. *Periodica Polytechnica Civil Engineering*, 65, 1050–1060.
- Thienel, K., Haller, T. 2020. Lightweight concrete - from basics to innovations. *MDPI Journal-Materials*, 13, 1–24.
- Unis, H., Mahmood, L.J., Muhammad, M.A., Faraj, R.H., Qaidi, S.M.A., Hamah, N., Mohammed, A.S., Mohammed, A.A. 2022. Geopolymer concrete as a cleaner construction material: An overview on materials and structural performances. *Cleaner Materials*, 5, 1–18.
- Zheng, Y., Zhou, N., Zhou, L., Zhang, H., Li, H., Zhou, Y. 2021. Experimental and theoretical study of bond behaviour between FRP bar and high-volume fly ash-self-compacting concrete. *Materials and Structures journal*, 54, 1–4.
- Zhou, L., Zheng, Y., Yu, Y., Song, G., Huo, L., Guo, Y. 2021. Experimental study of mechanical and fresh properties of HVFA-SCC with and without PP fibers. *Construction and Building Materials*, 267, 121010.